UPPSALA
UNIVERSITET

FYSMAST1069
Examensarbete 30 hp
Februari 2018

1kW Class-E solid state power amplifier for cyclotron RF-source

Stefan Book

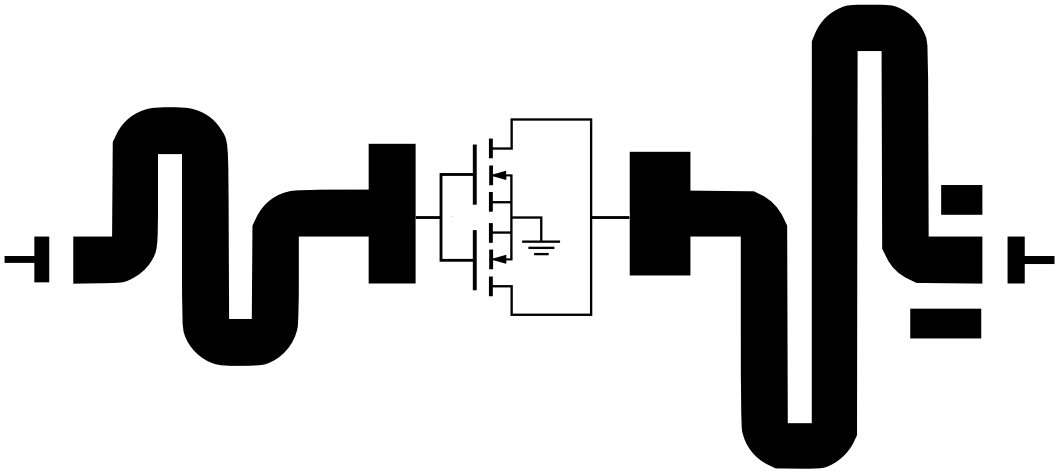

Masterprogrammet i fysik
Master Programme in Physics

UPPSALA
UNIVERSITET

Teknisk- naturvetenskaplig fakultet
UTH-enheten

Besöksadress:
Ångströmlaboratoriet
Lägerhyddsvägen 1
Hus 4, Plan 0

Postadress:
Box 536
751 21 Uppsala

Telefon:
018 – 471 30 03

Telefax:
018 – 471 30 00

Hemsida:
http://www.teknat.uu.se/student

Abstract

1kW Class-E solid state power amplifier for cyclotron RF-source

Stefan Book

This thesis discusses the design, construction and testing of a high efficiency, 100 MHz, 1 kW, Class-E solid state power amplifier.
The design was performed with the aid of computer simulations using electronic design software (ADS). The amplifier was constructed around Ampleon's BLF188XR LDMOS transistor in a single ended design.
The results for 100 MHz operation show a power added efficiency of 82% at 1200 W pulsed power output.
For operation at 102 MHz results show a power added efficiency of 86% at 1050 W pulsed power output.
Measurements of the drain- and gate voltage waveforms provide validation of Class-E operation.

Handledare: Dragos Dancila
Ämnesgranskare: Anders Rydberg
Examinator: Andreas Korn
FYSMAST1069

Contents

Abbrevations and Acronyms

AC	Alternating Current
dB	Decibel
dBm	Decibel-milliwatts
DC	Direct Current
GaAs	Gallium Arsenide
GaN	Gallium Nitride
HEMT	High Electron Mobility Transistor
HF	High Frequency
$\mathbf{I}_{DS}$	Drain Source Current
kW	Kilo Watts
LDMOS	Laterally Diffused Metal Oxide Semiconductor
MHz	Mega Hertz
PA	Power Amplfier
PCB	Printed Circuit Board
RF	Radio Frequency
$\mathbf{V}_{DS}$	Drain Source Voltage
$\mathbf{V}_{GS}$	Gate Source Voltage
$\mathbf{V}_{VSWR}$	Voltage Standing Wave Ratio

1 Sammanfattning

Effektförstärkare är en fundamental del av otaliga tillämpningar inom elektronik. Detta medför ett stort intresse i utvecklingen av effektförstärkare med hög uteffekt och samtidigt hög verkningsgrad, kompakt design och låg produktionskostnad.

En underkategori av effektförstärkare som är av speciellt intresse är switch-mode förstärkare där transistorn agerar likt en strömbrytare som diskret skiftar mellan ledande och oledande tillstånd. Denna kategori av effektförstärkare har potential att uppnå väldigt hög verkningsgrad genom att undvika samtidig ström och spänning i förstärkarens transistor.

Syftet med detta projekt är att designa, tillverka och mäta en switch-mode effektförstärkare i klass E med en uteffekt på 1000 watt och en driftfrekvens på 100 MHz.

Förstärkardesignen genomförs med hjälp av datorsimuleringar och sedan tillverkas den verkliga förstärkaren för hands. För att utvärdera förstärkarens prestanda mäts dess uteffekt, verkningsrad och förstärkningsfaktor.

Resultaten av detta projekt kan till exempel vara av intresse för partikelacceleratorer till vetenskapliga och medicinska tillämpningar.

Detta masterarbete är en del av Eurostarsprojektet ENEFRF, ett projekt riktat åt att utveckla energieffektiva effektförstärkare till cyclotroner.

En cyclotron är en typ av partikelaccelerator som kan användas till att accelerera protoner för att kollidera med syreatomer och därigenom producera radioisotopen fluor-18. Det radioaktiva fluoret sönderfaller främst med positronemission, och kan användas till positronemissionstomografi (PET). Genom att använda en fluor-18-baserad kontrastvätska kan man med PET avgöra plats och storlek hos cancertumörer i en patient [1].

2 Introduction

2.1 Background

Power amplifiers are a vital part of various electronics applications. For this reason there is considerable interest in developing power amplifiers with high power output while having high efficiencies, compact designs and low manufacturing costs.

A subcategory of power amplifiers of particular interest are switch mode power amplifiers. In a switch mode amplifier the transistor acts like a switch that alternates discreetly between being in a conducting or non-conducting state.

Switch mode amplifiers are of interest since they have the potential to reach high efficiencies by avoiding simultaneous current and voltage in the active device.

An example of applications where switch mode power amplifiers is of interest are for example in particle accelerators for use in science and medicine.

This master work is part of the Eurostars project: ENEFRF, a project aimed at developing energy efficient solid state amplifiers for cyclotron RF sources. A Cyclotron is a type of particle accelerator, which is frequently used to accelerate protons into oxygen atoms to produce the radioisotope fluorine-18. The radioactive fluorine decays primarily through positron emission, which allows it to be used in positron emission tomography (PET). Using a Fluorine-18 based tracer a PET scan can be used to determine location and size of cancerous tumours in a patient [1].

2.2 Methodology

The amplifier design procedure involves providing the transistor with input and output impedances that enables class E operation and fine tuning them for optimal performance.

To transform the load and source impedances into their optimal values at the gate and drain of the transistor; matching networks are designed and simulated.

The design and simulation of the matching networks and amplifier is performed using the electronic design software: Advanced Design System (ADS) by Keysight; in addition to the use of an ideal simulation model of the LDMOS transistor 'BLF188XR'[17] from Ampleon.

Based on the simulations a single ended amplifier has been designed, constructed and tested at the FREIA laboratory. The amplifier uses 2 parallel transistors encapsulated in a single package.

2.3 Objective

This master work aims to design, construct, and measure a 1 kW class E power amplifier; operating at 100 MHz, with high efficiency in a compact and simple design.

2.4 State-of-the-art

The field of power amplifiers is in continuous development with ever increasing demands on performance with regards to size, cost, heat tolerance, power, and efficiency.

When producing amplifiers the material properties of the transistor pose some limitations on performance. In order to meet these demands a multitude of competing transistor technologies have been developed using different semiconductor materials and device designs.

The three main technologies that make up the majority of high power RF amplifier transistors are: Silicon laterally diffused metal oxide semiconductor (LDMOS), Gal-

lium Arsenide (GaAs), and Gallium nitride (GaN). Each technology has individual strengths and weaknesses. Different regions of desired power output and operational frequency, per technology as follows:

- **LDMOS:** High breakdown voltage and power output capabilities, rugged (can handle large impedance mismatches/high VSWR), inexpensive. High output capacitance makes it less suitable for use at higher frequencies.
  Usage: High output power at low frequencies ($<$ 4 GHz [2]).
- **GaN:** High breakdown voltage, High power output capabilities even at high frequencies (low output capacitance). Expensive due to complicated manufacturing process.
  Usage: High output power at high frequencies.
- **GaAs:** Low breakdown voltage and low heat resistance leads to low power output capability ($>$50 W). Can operate at high frequencies.

  Usage: Low output power at low to high frequencies.

A table of published results for power amplifiers operating in frequencies of tens to hundreds of MHz is presented in table 1.

Year (ref)	**Class**	**P_{out} [W]**	**f [MHz]**	**η [%]**	**Duty cycle [%]**	**Technology**	**Architecture**
2016 [3]	AB	1250	352	71	5	LDMOS	Single-ended
2014 [4]	AB	2000	352	72	20	LDMOS	Push-pull
2010 [5]	E	145	85-120	86	100	LDMOS	Single-ended
2010 [6]	AB	104-121	100-1000	69-79	100	GaN HEMT	Push-pull
2016 [7]	F^{-1}	300	10.1	74	100	GaN HEMT	Single-ended
2016 [8]	AB	700	400-500	75	15	GaN HEMT	Push-pull
2017 [9]	B	1000	420-450	70	10	GaN HEMT	Single-ended
This work	E	1050	102	87	5	LDMOS	Single-ended

Tab. 1: Performance overview of published power amplifiers.

For the amplifier design in this work an LDMOS transistor was chosen due to its high breakdown voltage, power output capability and ruggedness.

3 Theory

This section will assume that the reader is familiar with some concepts of microwave engineering such as: Transmission lines, reflection coefficients, the Smith-chart, impedance matching, and scattering parameters. For a brief overview of these subjects, see appendix B.

3.1 RF power amplifiers

An RF power amplifier can be seen as consisting of a few distinct parts. Namely, The input matching network, the transistor, the output matching network and the bias network. A diagram of the basic structure of a power amplifier is presented in fig 1:

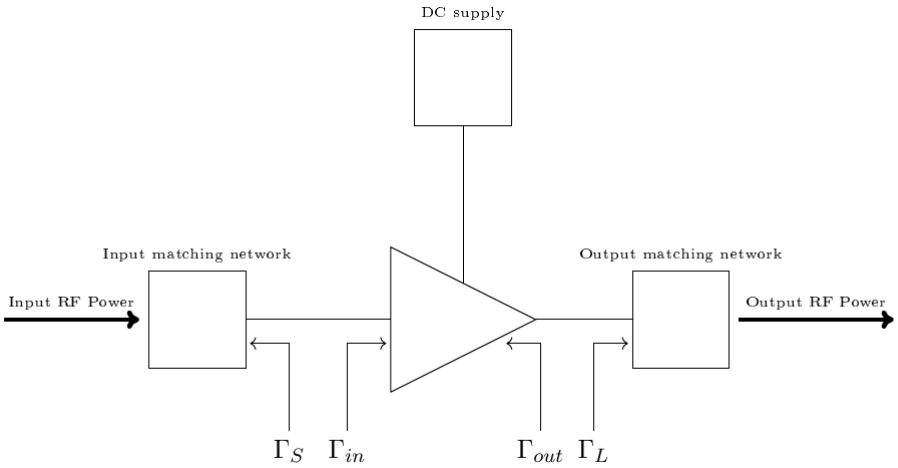

Fig. 1: Schematic diagram of an RF power amplifier.

The reflection coefficients of the transistor input and output are denoted Γ_{in} and Γ_{out}, and the coefficients for the source and load are denoted Γ_S and Γ_L respectively.

The source and load are typically 50 Ohms which is generally not the same as the input and output impedance of the transistor. Therefore we utilize matching networks on the input and output to match the impedances of the source and load to the desired impedances (i.e. reflection coefficients) at the input and output of the transistor.

The DC-bias networks supply the amplifier with DC power that is to be converted to RF output power. It also provides the biasing conditions to allow the transistor to operate with the desired gate-source voltage.

The efficiency of the amplifier is the ratio between output RF power and the supplied DC power:

$$\eta = \frac{P_{out}}{P_{DC}} \tag{1}$$

Though, there are numerous different measures of efficiency, and another commonly used measure is the power added efficiency which takes into account the RF power supplied to the amplifier.

$$PAE = \frac{P_{out} - P_{in}}{P_{DC}} \tag{2}$$

The power added efficiency is often a more suitable measure of an amplifiers efficiency, since neglecting the input power is rarely useful. This is especially true at lower gains, where the effects of neglecting input power are more significant.

3.2 Stability

The stability of an amplifier describes its resilience towards self induced oscillations. These oscillations can occur if a voltage seen at the output induces a voltage at the input. This type of feedback behavior gets amplified due to the voltage gain of the amplifier and causes unwanted oscillations.

An amplifier can be either conditionally or unconditionally stable. An unconditionally stable amplifier will remain stable regardless of what impedance it sees on the source and load.

A conditionally stable amplifier will only be stable for a subset of source and load impedances.

The stability of an amplifier can be determined analytically using S-parameter values. The s-parameters of the amplifier can be used to calculate two measures of stability K and Δ

An amplifier is unconditionally stable if both $K > 1$ and $|\Delta| < 1$.

Where K and $|\Delta|$ are described by the following equations[15]:

$$K = \frac{1 - |S_{11}|^2 - |S_{22}|^2 + |\Delta|^2}{2|S_{21}S_{12}|} \tag{3}$$

Where the Δ is described by:

$$\Delta = S_{11}S_{22} - S_{12}S_{21} \tag{4}$$

Since the S-parameters of an amplifier is frequency dependent, so is the measures of stability. That is to say an amplifier may be unconditionally stable for some frequencies and simultaneously be conditionally stable for others.

3.3 Classes of operation

Amplifiers are generally classified according to which class of operation the transistor is operating in. The classes of operation can be divided into transconductance classes and Switch-mode classes.

The transconductance classes, A, AB, B and C are classified according to their conduction angle. The conduction angle of an amplifier is the part of a gate voltage signal for which the transistor is conducting, and is determined by the biasing conditions of the transistor.

- A Class A power amplifier is biased to conduct for the entire period of the input signal. And thus has a conduction angle of 360° Since it is always conducting, there is current constantly flowing through the device resulting in significant losses. It has a theoretical maximum efficiency is 50% [16].
- A Class B amplifier is biased so that it is balancing on the threshold voltage, any positive voltage on the input will cause conduction and as such it has a conduction angle of 180°. It has a theoretical maximum efficiency is 78.5% [16].
- A Class AB amplifier is biased somewhere in between class A and class B and consequently has a conduction angle between 180° and 360°. And it has

theoretical efficiencies between 50% and 78.5%

- A class C amplifier is biased so that the conduction angle is less than 180° Smaller conduction angle gives less quiescent current losses. It is capable of higher theoretical efficiency than class B but suffers from lower gain.

Switch-mode classes like class D and E are not really defined by their biasing. Instead the transistor is operated like a switch that jumps back and forth between cutoff and saturation. Ideally switch-mode amplifiers are driven using input voltage to facilitate fast switching.

The main advantage of switch mode classes is that the transistor is either entirely conducting or entirely non-conducting. This ensures low losses since it leads to no simultaneous voltage and current in the device. Since while the transistor is on there is a large current but low a voltage, and when the transistor is off there is a high voltage but a low current in the device [16].

3.3.1 Biasing and conduction angles

For practical reasons it one might choose to not use a square wave voltage at the input for a switch mode amplifier. When using a square wave input signal the conduction angle is just the duty cycle of the square wave signal.

If we instead assume a sinusoidal voltage and we wish to achieve a certain conduction angle, a DC-offset can be applied to the signal.

Assume that conduction occurs for all positive voltages and that the input signal is on the following form:

$$V_{in} = A \cdot sin(\omega t)$$

If a DC-bias $A \cdot \epsilon$ is added, the signal becomes:

$$V_{in\epsilon} = A \cdot (sin(\omega t) + \epsilon)$$

The relationship between added DC bias and conduction angle is illustrated in figure 2 . Three voltage signals are plotted for the cases of positive, zero, and negative DC-bias.

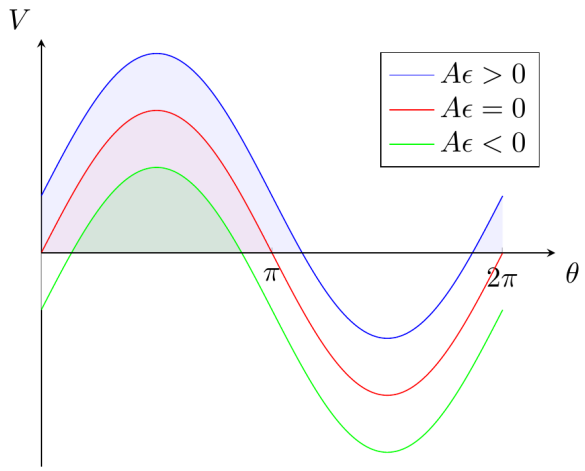

Fig. 2: Sinusiodal voltage signals, each with a different DC-bias Aϵ. The conducting part of each signal is shaded.

The problem of when an ideal voltage switch is conducting for a DC-offset sinusoidal input voltage can be reformulated into the geometrical problem of finding a relationship between θ_{CA} and ϵ in the image below:

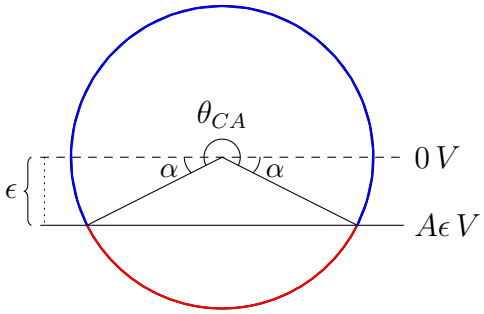

It can be seen that:

$$\epsilon = \sin(\alpha) \implies \alpha = \arcsin(\epsilon)$$

The angle α is readily expressed in terms of the conduction angle:

$$\alpha = \frac{\theta_{CA} - \pi}{2}$$

This gives the following relationship between ϵ and θ_{CA}:

$$\pi + 2\arcsin(\epsilon) = \theta_{CA}$$

3.4 Class E

As a switch mode amplifier, the objective of a class E amplifier is to separate voltage and current in the transistor. This is the main idea behind using the transistor as a switch. While the switch is closed, the current flows through the switch, but it has no resistance and therefore there is no voltage drop over the switch. While the switch is open there is a voltage drop over the switch but there is no current flowing. Losses in the transistor occur only when voltage and current waveforms overlap, since the power dissipated is the product of the voltage and current in the device [19].

A schematic of an ideal class E amplifier can be seen in figure 3.

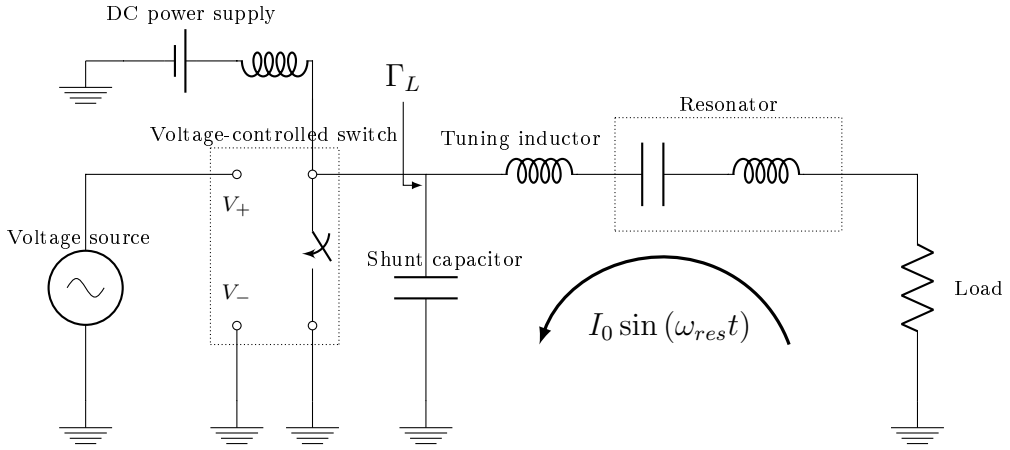

Fig. 3: Schematic diagram of an ideal class E circuit.

An ideal class E amplifier can be divided into a few basic parts which have been labeled in the above image. The circuit consist of a voltage controlled switch which is turned ON and OFF by a voltage source at the input. The output side of the switch is connected to a DC-power supply, and to the output circuit, which in turn is connected to the load.

The output circuit consists of three parts:

- The resonator consisting of a inductor and a capacitor. It acts as a band pass filter, which transmits the resonant frequency but filters out harmonics.
- The shunt capacitor which allows current to be drawn from ground while the switch is open.

- Tuning inductor which ensures zero voltage switching.

The operation of an ideal class E amplifier can be summarized as follows:

If there is a positive voltage on the input the switch is closed. When the switch is closed the resonator pulls current through the load and into the switch. If there is a negative voltage on the input the switch is open. When the switch is open the resonator pulls current through the shunt capacitor and into the load.

The resonator filters out any harmonic content, so that all power transmitted to the load is at the fundamental frequency. The harmonics help to shape the drain voltage waveform at the transistor which is responsible for the high efficiency of the class E amplifiers [16].

The tuning inductor is used to achieve the correct phase shift of the drain voltage. This ensures that the drain voltage is zero when the transistor closes and drain current begins to flow . This ensures that the losses in the transistor are low.

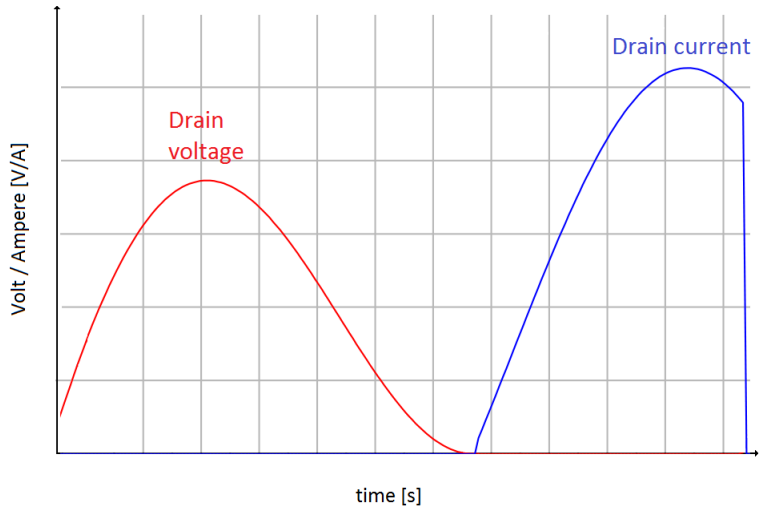

Fig. 4: Schematic illustration of ideal class E current and voltage waveforms.

Fig. 5: Schematic image of the ideal drain voltage and drain current waveforms of a Class E amplifier.

The benefit of the class E design is the possibility of very high efficiency. Conversely, its main drawback is that the drain voltage peaks are large, and in theory they could become up to 3.56 times as large as the DC drain bias voltage [16]. This causes the

breakdown voltage of the transistor to become a limiting factor when designing class E amplifiers.

The set of equations that relate the operation of an amplifier to its components is known as its design equations. The design equations for class E amplifiers were reported by N. Sokal in 1975 [10]. Some examples of the equations are presented below:

$$R_{load} = \frac{(V_{cc} - V_{Th})^2}{P_{out}} \tag{5}$$

$$C_{shunt} = \frac{1}{\omega R_{load} \cdot 5.447} \tag{6}$$

$$L_{tune} = \frac{1.1525 \cdot R_{load}}{\omega} \tag{7}$$

However, these equations assume a 50% duty cycle, and it is not necessarily the duty cycle that will ensure optimal performance in any given design.

Equations that take duty cycle into account were published by Raab in 1977 [11]. However they are cumbersome and usually used in graphical a format or computer templates rather than in explicit form.

4 Design and Simulation

The measurement equations used in the ADS simulations are displayed in Appendix A

4.1 The transistor: Ampleon BLF188XR

The transistor used for the amplifier is an LDMOS power transistor from Ampleon named BLF188XR [13]. In each unit casing there are two transistors. Each transistor has a maximum drain source current of 77 amperes and a maximum drain source voltage of 135 volts. The choice of this transistor is due to it having high gain and tolerating high voltage peaks and currents without degradation.

4.2 Frequency of operation

The choice of operational frequency was the highest possible from a set of frequencies of interest, considering the transistor. The frequencies all relating to application in particle accelerators.

Initially, simulations of class E amplifiers were made for the frequencies 352 MHz and 704 MHz but did not yield functioning circuits.

The reason for this is that the output capacitance of the transistor (212 pF) limits the maximum operating frequency.

The maximum operating frequency of an optimal class E amplifier is given by the expression [16]:

$$f_{max_E} = \frac{I_{max}}{56.5 C_{out} V_{cc}} \approx 130 \text{ MHz}$$

Above this frequency-threshold efficiency will start to suffer since the drain voltage waveform is limited by the charging of the output capacitance.

Using the maximum values for our transistor we get a theoretical frequency limit of approximately 130 MHz. This confirmed the decision to realize a 100 MHz amplifier.

This maximum frequency of class E operation should not be confused with the frequency of unity gain for the transistor, commonly denoted f_{max}. which is higher. For the BLF188XR the frequency of unity gain was found to be about 700 MHz in simulation with V_{gs} =2 V and V_{ds} = 45 V.

4.3 Lumped component circuit

The amplifier is designed using the class E design equations from Raab [11], which result in a circuit composed of lumped components.

A template that implements the design equations in ADS was used [18]. The design equation template is displayed in figure 6.

The subsections of the template have been numbered, their functions are:

1. Allows the user to enter the following device parameters and limits:
   - $\mathbf{V}_{max}$ - The maximum allowed drain voltage peaks.
   - $\mathbf{I}_{max}$ - The maximum allowed drain current peaks.
   - $\mathbf{C}_{intrinsic}$ - The output capacitance of the transistor (C_{DS}).
   - $\mathbf{V}_{knee}$ - The knee voltage of the transistor. (Found from DC-simulation).
   - $\mathbf{I}_{DC-max}$ - Maximum allowed DC drain current.
2. Allows the user to choose the following circuit parameters:
   - Frequency of operation.
   - DC-supply voltage (Drain bias).
   - Output power.
   - Conduction angle (θ_{CA}).
3. Displays the component values of the synthesized circuit.

4. Displays waveforms, peak drain voltage and -current values, and circuit values.

   (a) Displays the drain voltage and -current waveforms of the synthesized circuit.

   (b) Displays the peak value of drain voltage as a function of conduction angle. Higher conduction angles leads to higher drain voltage peaks, so the maximum allowed drain voltage sets an upper bound for θ_{CA}.

   (c) Displays the peak value of drain current as a function of θ_{CA}. Lower θ_{CA} leads to higher drain current peaks, so the maximum allowed drain current sets a lower bound for θ_{CA}.

   (d) Displays the shunt capacitance value a function of θ_{CA} The bounds on θ_{CA} mark the range of shunt capacitance values that produce a reliable circuit.

   (e) Displays the values of the tuning inductor and the load resistance as a function of θ_{CA}. The bounds on θ_{CA} mark the range of values that produce a realiable circuit.

   (f) Displays the values of the resonator capacitance and inductance as a function of θ_{CA}. The bounds on θ_{CA} mark the range of values that produce a reliable circuit.

A single ended design was constructed in ADS using a simulation model of the BLF188XR transistor and lumped components calculated from the design equations.

The ADS simulation setup for the lumped component circuit can be seen in figure 7.

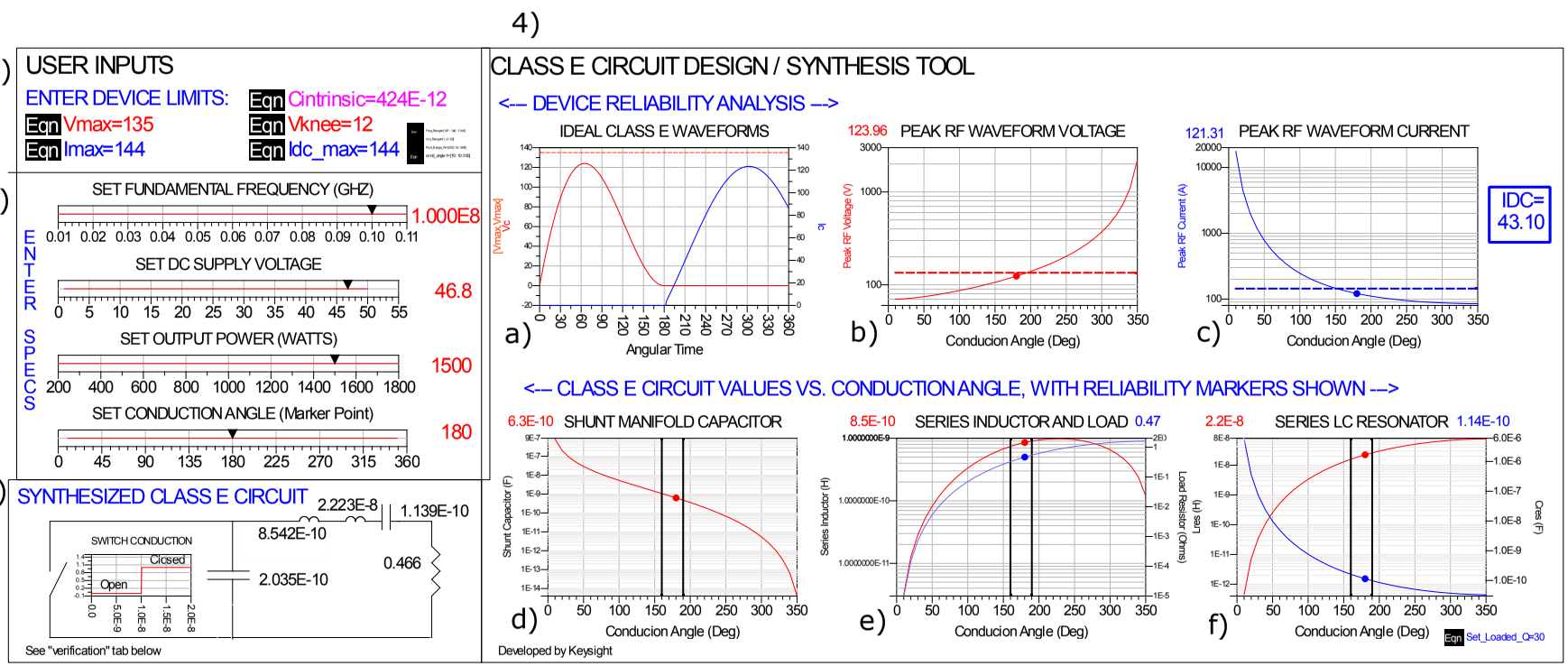

Fig. 6: ADS design equation template.

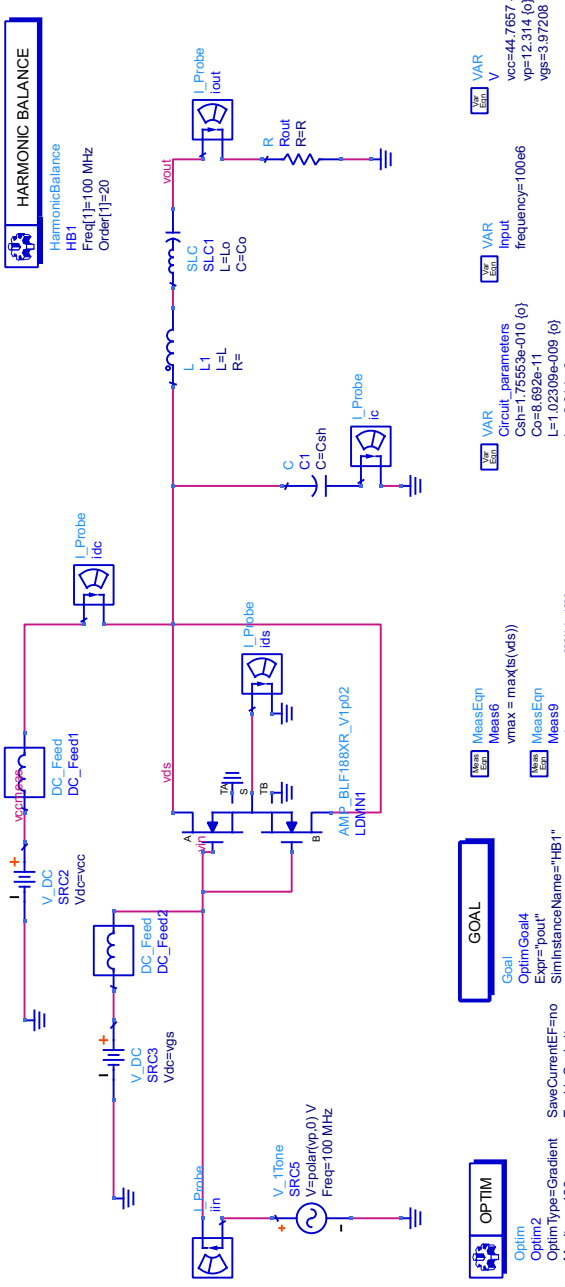

Fig. 7: Simulation setup for the lumped component circuit.

The design equations provide a good starting point for the circuit, but they assume a perfect voltage switch as a transistor and as such the circuit needs to be tuned to accommodate the differences that arise from using a more realistic transistor model.

Once lumped circuit component values have been found that give satisfactory performance, the impedance seen at the output of the transistor is determined. The output impedance is used as a target for constructing the circuit using transmission lines.

The simulated waveforms of the lumped component circuit can be seen in figure 8 and the overall simulation results are displayed in table 2.

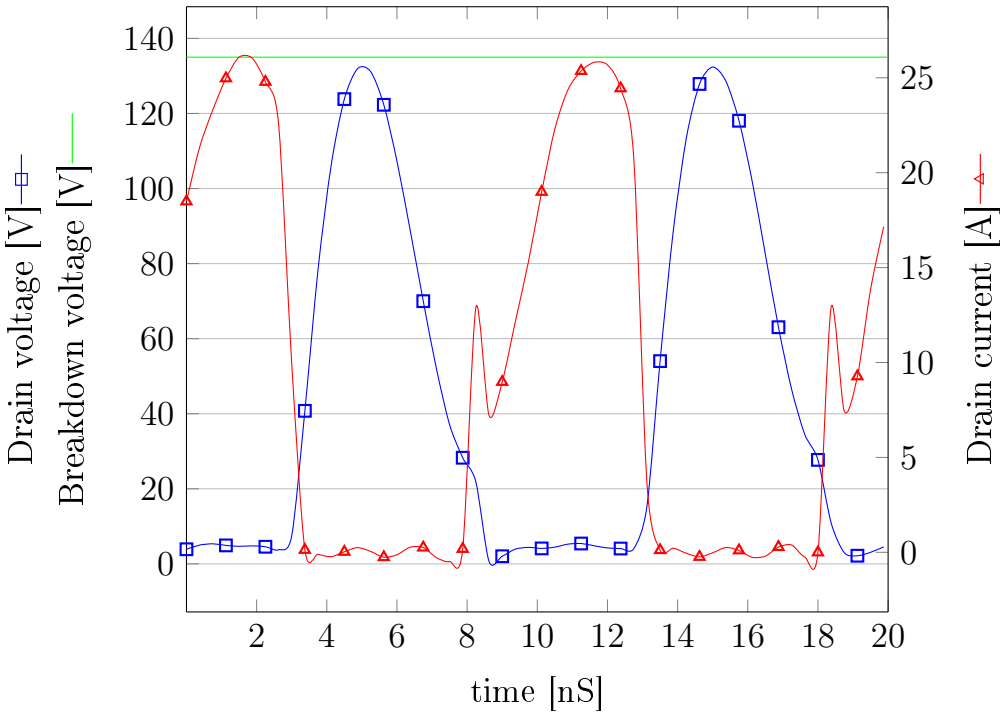

Fig. 8: Simulated drain voltage and drain current waveforms for the lumped component simulation.

PAE	P_{out}	P_{DC}	$Max(V_d)$
88.2 %	1480 W	1664 W	132 V

Tab. 2: Simulation results for the lumped component circuit

4.4 Design using transmission lines

After the impedance using lumped components is established, a design using ideal transmission lines can be devised. The aim is now to construct the target impedance using only transmission lines and shunt capacitors.

The circuit is designed by matching the target impedance at the output to the 50Ω impedance of the load. To achieve this matching a Smith chart was used. The matching is performed adding transmission lines and shunt capacitors as a way to move in the Smith chart.

Once the circuit is constructed component values could be tuned to further improve the performance.

Once a circuit using ideal transmission lines has been produced the next step is to perform simulations using more realistic transmission lines; since effects such as losses and the influence of a substrate needs to be considered.

The tool 'MLIN' in ADS allows for the simulation of microstrip lines including choice of substrate parameters.

To achieve the desired performance the circuit values are optimized using the optimization tool in ADS.

The optimization tool in ADS allows the user to automatically optimize the performance of a circuit using a set of user defined optimization goals. The tool attempts to iteratively find a solution based on the optimization goals by sweeping chosen variables incrementally, such as component values.

The transmission line circuit was optimized by varying the dimensions of the transmission lines, the values of shunt and DC-block capacitors, gate and drain biases, input power and RF choke inductors.

Using goals of 1500 W output power, 90% power added efficiency and shunt capacitor voltages below 500 V. All of the goals will not realistically be reached, but are chosen to push the solution in a desired direction. The goals were chosen to prioritize power added efficiency.

The resulting simulated circuit can be seen in image 9. The full input and output matching networks are not included in the image since they are way too big.

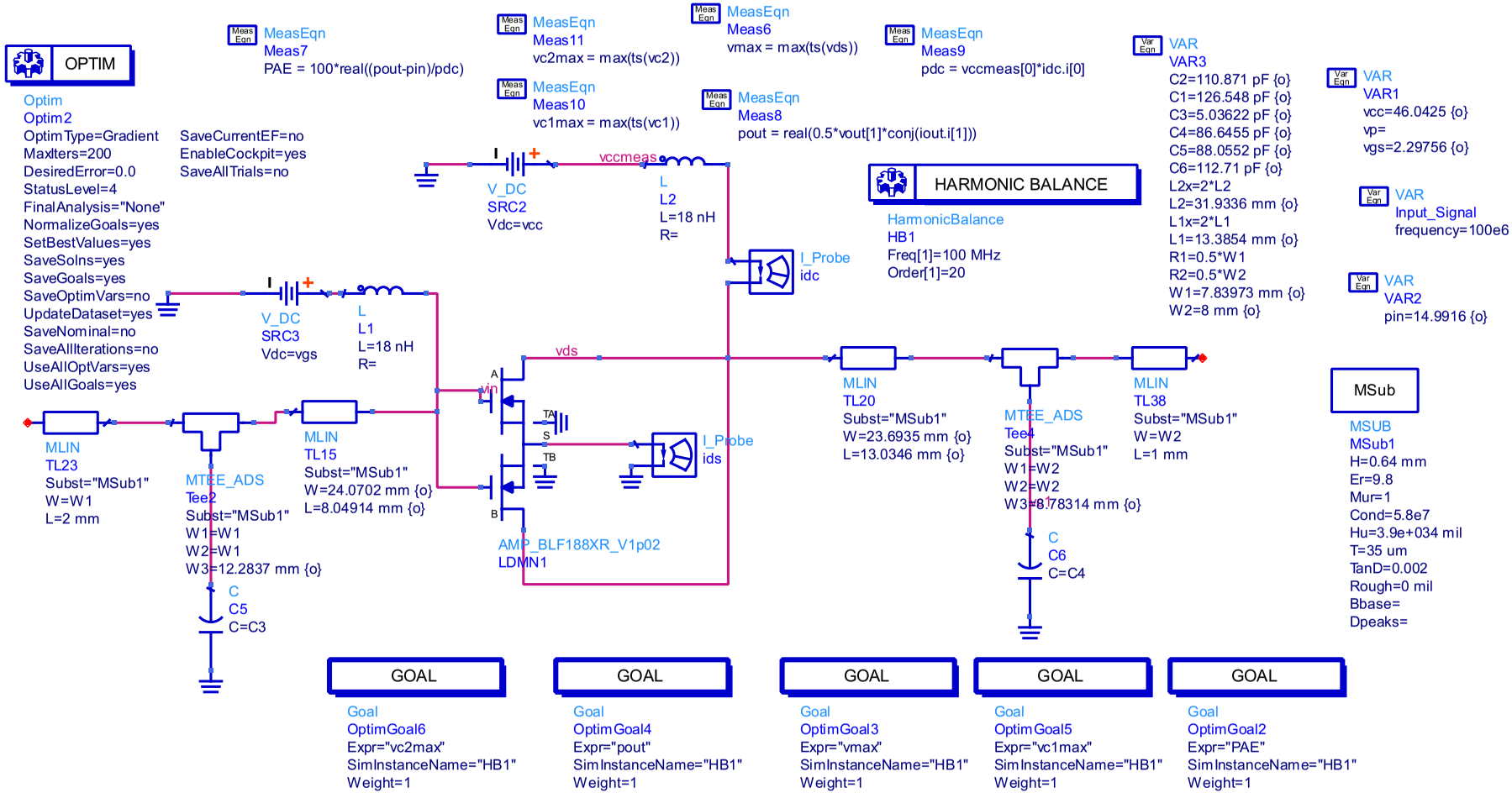

Fig. 9: Simulation setup for the microstrip circuit.

After the optimization of the realistic transmission lines the results in table 3 were found.

PAE	P_{out}	P_{DC}	$Max(V_{ds})$	$Max(V_{C1})$	$Max(V_{C2})$
83.2 %	1415 W	1702 W	131 V	128 V	460 V

Tab. 3: Simulation results for the microstrip circuit.

Compared to simulations using ideal lumped components the efficiency of the simulated amplifier has decreased, which is to be expected since the microstrip simulation takes into account losses in the transmission lines.

4.5 Momentum simulations

The electromagnetic fields produced during operation of the amplifier give rise to effects that could affect its performance. For instance there could be capacitive coupling between the transmission lines and the surrounding ground plane of the amplifier.

In order to take these effects into consideration the electromagnetic fields of the operating amplifier needs to be simulated in beforehand.

To simulate the electromagnetic fields a complete model of the amplifier needs to be constructed including the type and dimensions of the substrate, the copper thickness, ground planes, etc.

The momentum simulator uses numerical computational methods to solve the partial differential equations that describe electromagnetic field, which are Maxwell's equations.

After the momentum simulation circuit has been optimized to achieve ideal performance the simulation part of the design process is complete.

Figure 10 depicts the momentum simulation circuit in ADS, table 4 shows the simulation results, and figure 11 displays the simulated drain current and -voltage waveforms.

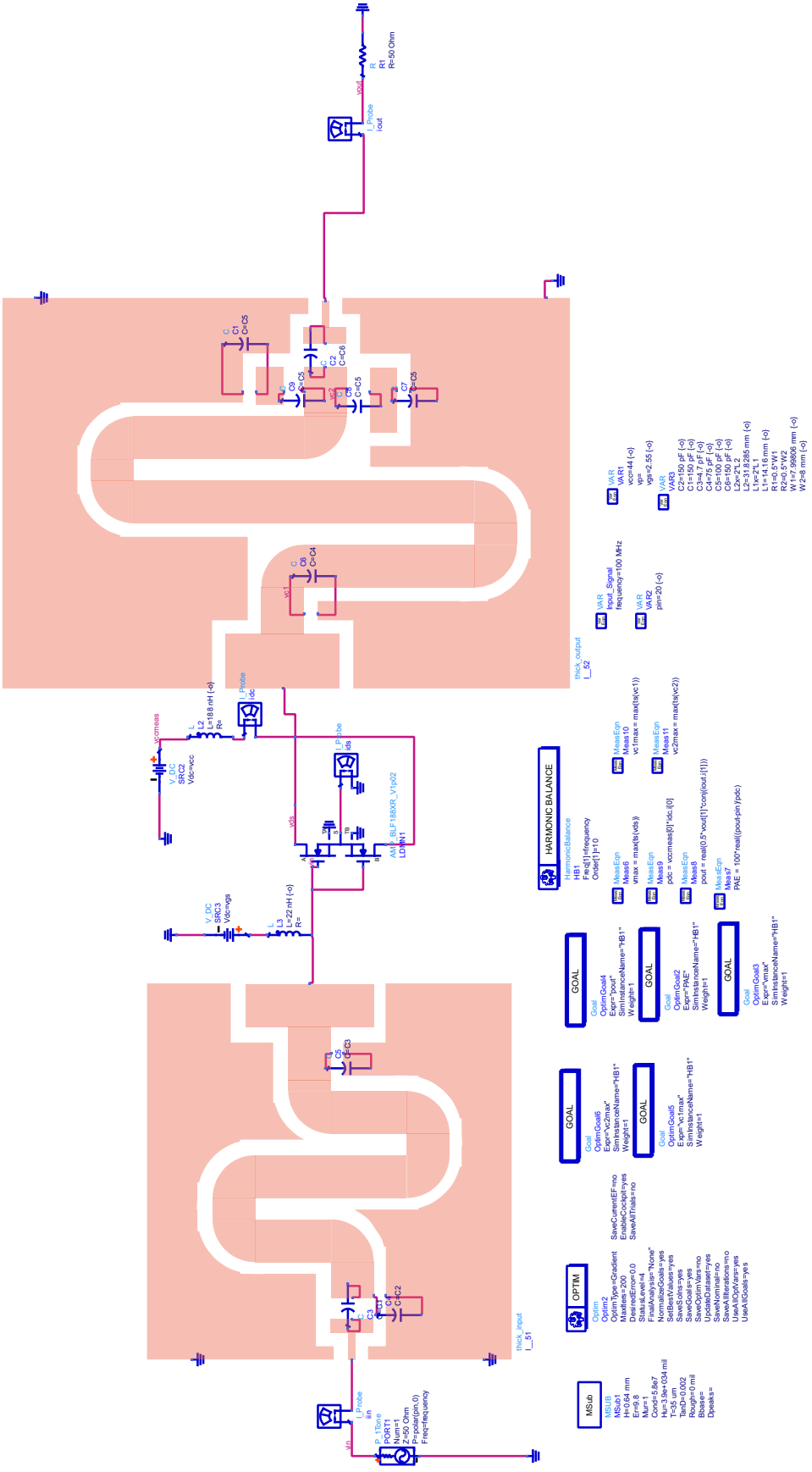

Fig. 10: Simulation setup for the momentum circuit.

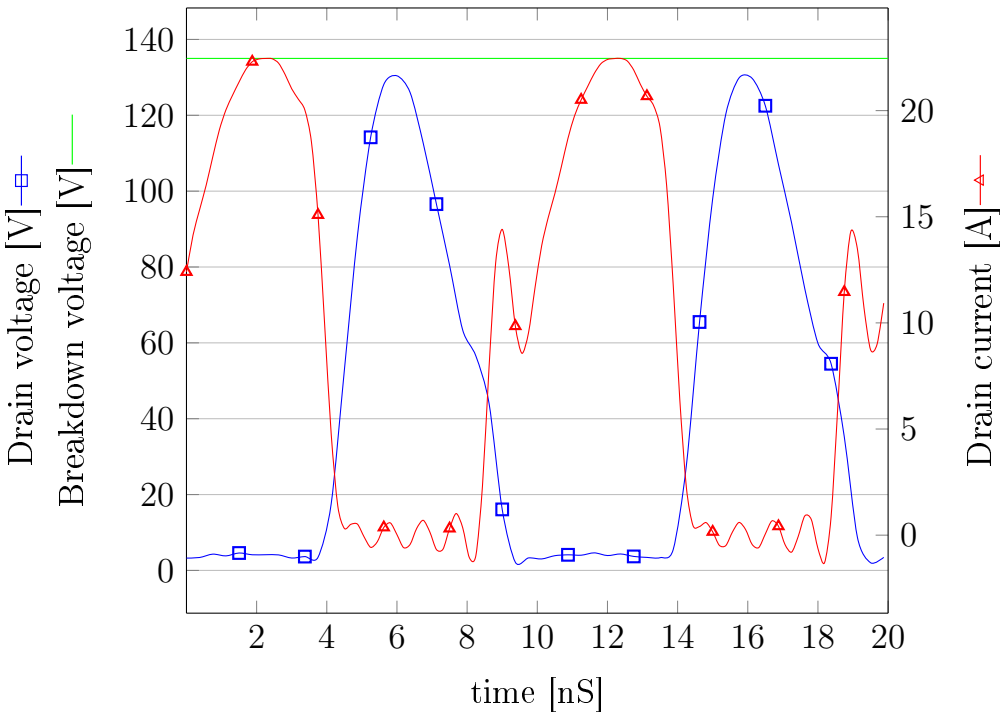

Fig. 11: Simulated drain voltage and drain current waveforms for the momentum simulation.

PAE	P_{out}	P_{DC}	$Max(V_{ds})$	$Max(V_{C1})$	$Max(V_{C2})$
75.8 %	1330 W	1730 W	131 V	105 V	417 V

Tab. 4: Simulation results for the momentum circuit.

4.6 Stability analysis

To determine the conditions of stability of the transistor a stability simulation was performed. A stability simulation consists of simulating the S-parameters of an amplifier circuit over a range of frequencies and calculating the the stability parameters K and $|\Delta|$ at each frequency.

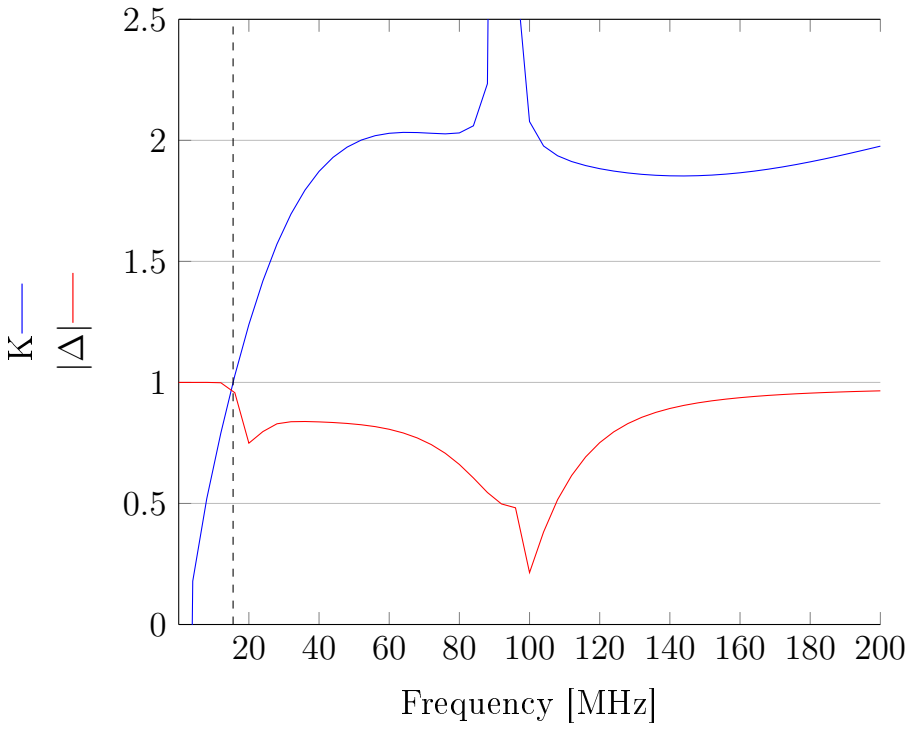

Fig. 12: Simulated stability parameters for the MLIN simulation circuit.

From the stability simulation in figure 12 we can see that both conditions for unconditional stability are fulfilled at the design frequency of 100 MHz. The transistor will be conditionally stable at frequencies of 15 MHz or lower since the stability factor K drops below 1.

A way of ensuring unconditional stability below 15 MHz is to add a resistor to ground at the transistor input [12]. This was however overlooked at the time of circuit design.

5 Amplifier construction

The circuit board used for the amplifier was produced by hand using an etching method. From the momentum simulation a profile of the circuit was acquired. By printing this profile on photo-paper and laminating it to the circuit board, the ink is transferred to the circuit board. The entire circuit board is then submerged in the etching solution and the copper that is not covered by the ink mask is etched away.

The substrate used to create the circuit board is a 0.64 mm double-sided copper clad Rogers TMM10i. It was chosen primarily for its high electrical permitivity, but also for its tolerance to heating [20].

Property:	Typical value:
Dielectric constant, ϵ_r	9.8 ± 0.245
Dissipation factor, $tan(\delta)$	0.0020
Dielectric thickness	0.635 mm
Copper thickness	35μm

Tab. 5: Table of substrate parameters for Rogers TMM10i.

The high electrical permitivity ensures that the circuit can remain relatively small. Considering that at 100 MHz transmission lines tend to be quite large.

The substrate has copper layers on both sides with thicknesses of 35 μm. The bottom layer is left unectched and serves as a ground plane.

The circuit is designed to have ground planes on the top layer, surrounding the transmission lines. In order to create a connection between the bottom and top ground planes; 1 mm diameter holes were drilled through the PCB and conductors were soldered through the holes on both sides of the PCB. This process is known as viasing and is a common technique for connecting two sides of a PCB.

After the viasing was performed the bottom side of the PCB was covered in solder to ensure a good connection between the viasing and the ground plane. The solder was then sanded flat in order to allow the circuit board to lie flush against the heat sink.

Once the circuit board was prepared, the lumped components for the amplifier such as capacitors, inductors and the transistor could be soldered by hand.

The circuit design allows for moving capacitors along the transmission lines for future tuning.

The capacitors used are Cornell Dublier mica capacitors with a rated maximum voltage of 300 volts. However, the simulated voltage drop over the second output capacitor is about 420 volts.

To solve this issue the second output capacitance is produced with the use of 4 capacitors, namely two serially connected pairs of parallel capacitors. This setup has the same capacitance as a single capacitor of the same value, but has the benefit that each individual capacitor only experience half the voltage drop. The four capacitor setup can be seen in figure 13, each capacitor marked C2.

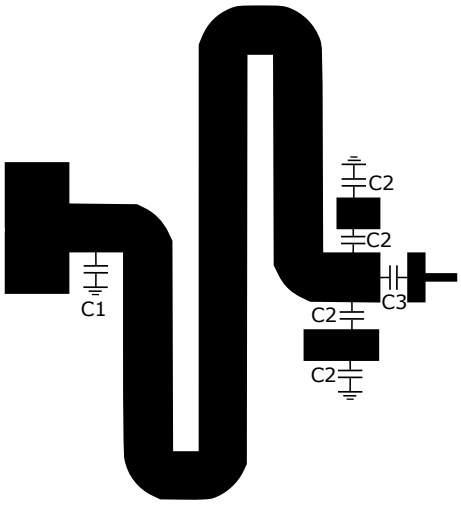

Fig. 13: Output circuit schematic with enumerated capacitors.

The circuit board has two DC bias inputs equipped with filter capacitors and RF choke inductors. One is for providing the gate bias on the input and one is for providing the DC power at the output.

The RF choke inductance for the output DC bias was chosen to be 200 nH and was hand wound from 1.5 mm copper thread. The inductance was calculated using the software Coil32. The inductance of the choke should be chosen as to have a high impedance at the operating frequency. It could have been chosen higher since 200 nH corresponds to 126 Ω at 100 MHz.

During operation of the amplifier heat will dissipate in the transistor, therefore the amplifier will need to be cooled while running.

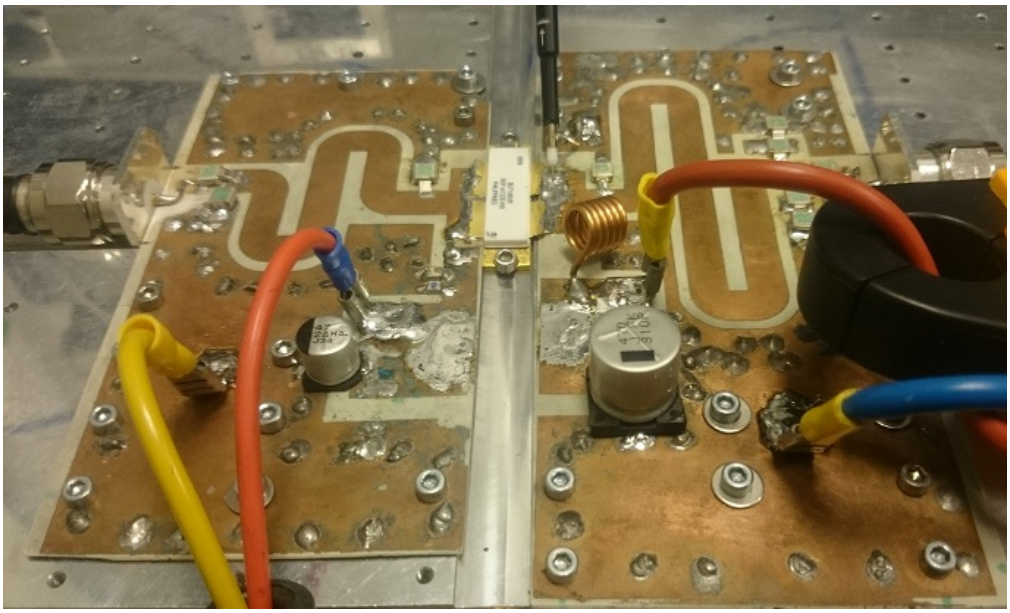

Fig. 14: Fully assembled amplifier mounted on the heatsink.

The cooling of the amplifier is performed by mounting the amplifier on a heatsink. The heatsink consists of a block of aluminum which is fitted with a water pipe running through it. This enables for water cooling at a flow rate of 8 l/min. The finished amplifier can be seen in figure 14.

6 Measurement setup

The performance of the amplifier is measurement with the setup in figure 15. The setup measures the incoming and outgoing power of the amplifier and the DC-power provided during operation. This allows for calculating the power added efficiency.

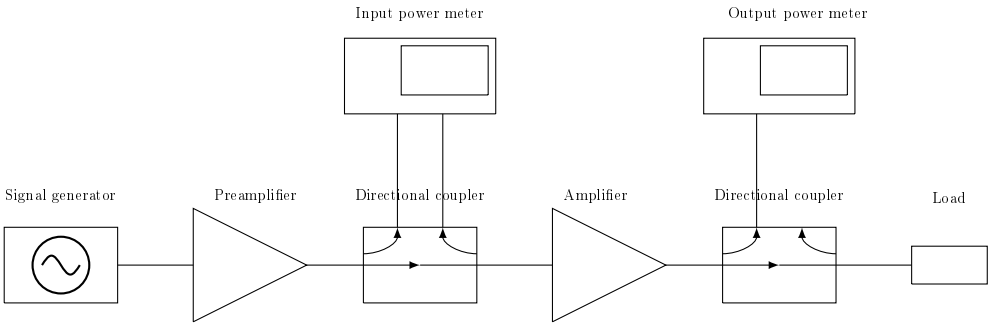

Fig. 15: Schematic diagram of the power measurement setup.

The signal generator provides a 100 MHz voltage signal which is amplified using a 100W pre-amplifier. The signal generator was used to provide signal powers between -20dBm and -8 dBm. At 100 MHz the pre-amplifier amplifies the signal with 50dB resulting in input power of 30 dBm to 42 dBm (1-16 W).

To measure how much of the signal is transmitted and reflected at the input a directional coupler is inserted between the pre-amplifier output and amplifier input. The directional coupler couples a small fraction of the power delivered to the load to a power meter. Similarly, but to measure reflection and transmission at the load a directional coupler is inserted between the amplifier output and the 50 ohm load.

Two independent power supplies were used to produce the DC-biases for the gate and drain. The DC supply voltage for the drain bias was experimentally determined to 45 volts, observing the magnitude of the drain voltage peaks and increasing the DC-voltage until the peaks were approaching the breakdown voltage of the transistor (135 V). This results corresponds well to the simulated DC supply voltage of 44 V.

The DC supply voltage of the gate bias was experimentally determined by gradually increasing the voltage whilst keeping the drain current stable. If too high gate voltage was applied the drain current increased continually. The gate voltage used was 1.75 V, quite a bit lower than the simulated 2.55 V. The difference could be

due to discrepancies between the simulation model of the transistor and the physical transistor.

In order to measure the efficiency of the amplifier the DC-power provided needs to be measured. The DC-current supplied to the output was measured using a current probe connected to an oscilloscope. The probe is depicted in figure 16.

Fig. 16: Current sensor used to measure the drain current.

The efficiency of the amplifier could be calculated using equation 2.

The signal provided to the amplifier during the power measurements consists of a pulsed sinusoidal voltage of 3.5 μs pulses between delays of 66.5 μs for a total period of 70 μs resulting in a duty cycle of 5 %.

The voltage waveforms at the drain and gate were measured using an oscilloscope and two high voltage probes.

7 Measurements and results

7.1 100 MHz performance

The gain and efficiency of the amplifier was measured for output powers from 100 W to 1200 W.

Figure 17 displays the power added efficiency of the amplifier versus output power and figure 18 displays the gain of the amplifier versus output power.

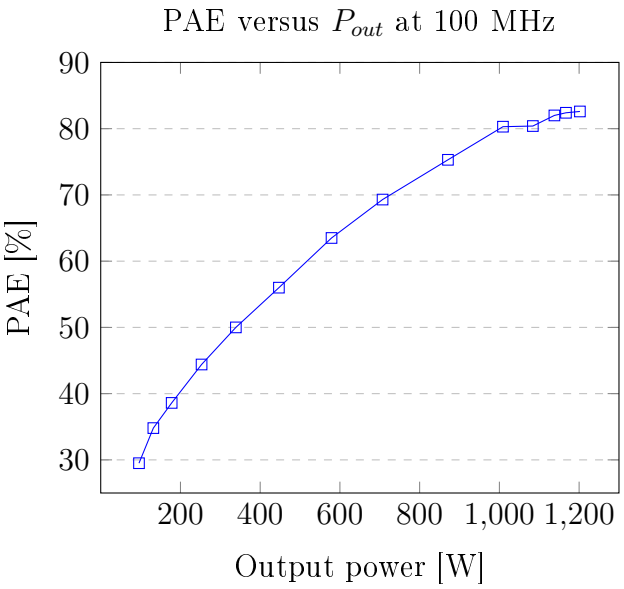

Fig. 17: Power added efficiency as a function of output power measured at 100 MHz

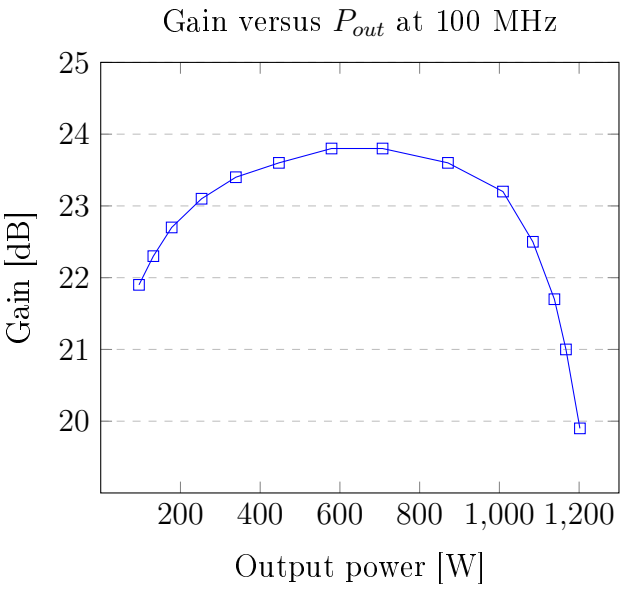

Fig. 18: Power gain as a function of output power measured at 100 MHz

The results are close to what was expected from simulations with a maximum power added efficiency of 82.6% at an output power of 1202 W.

The drain voltage waveform was measured as well and is displayed in figure 19.

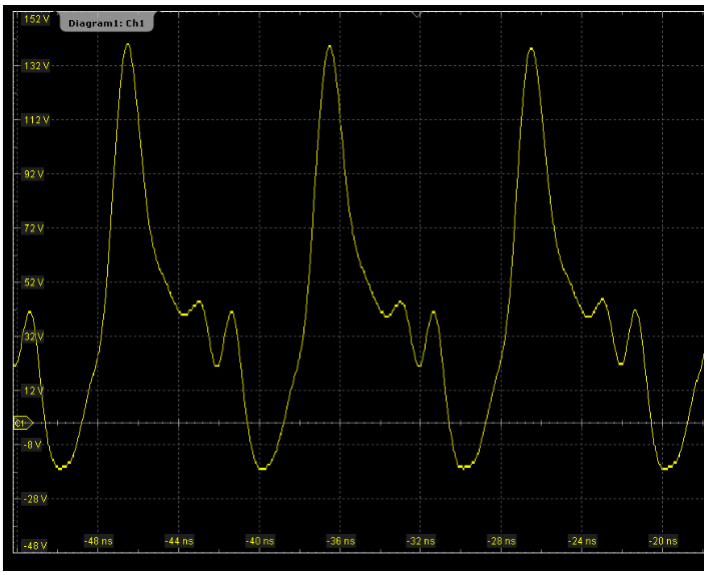

Fig. 19: Measured drain voltage waveform at 100 MHz

The waveform looks similar to simulations except that the voltage dips below zero

in between peaks and the hump shortly after the main peak.

The discrepancies between measured and theoretical drain voltage waveforms are the result of a slight impedance mismatch at the output, leading to reflections that would influence the shape of the waveform. The reason for the mismatch could be that the resonator is not quite tuned to 100 MHz.

In order to test this hypothesis the drain voltage waveform was measured for a range of frequencies surrounding the design frequency. (97-105 MHz).

Figure 20 shows the measured drain voltage waveforms at different frequencies.

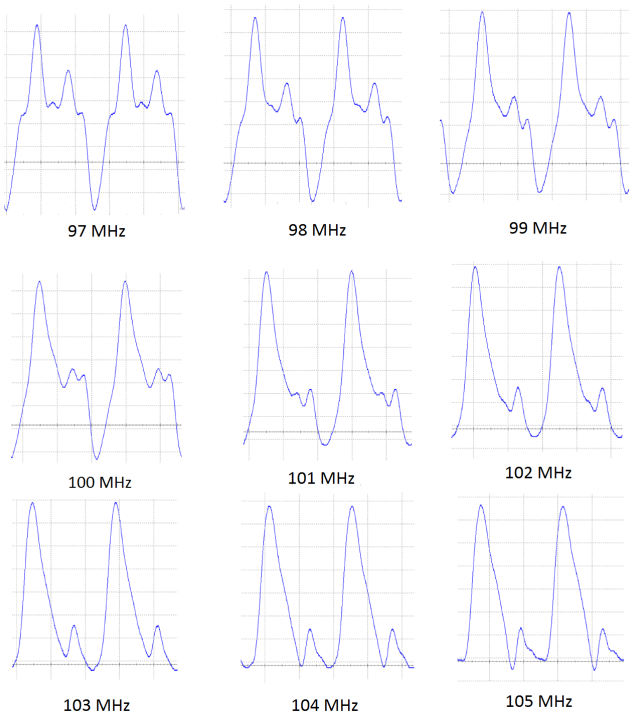

Fig. 20: Measured drain voltage waveforms from 97 to 105 MHz

At lower frequencies there is a pronounced secondary peak in the drain voltage. For increasing frequencies the second peak diminishes. The tendency for the voltage to dip to negative values in between peaks also diminished with increasing frequencies and at about 102 MHz the voltage goes to zero.

The waveforms at 102-103 MHz correspond better to the simulations. Confirming that the resonator is not perfectly tuned to 100 MHz.

The output power and power added efficiency was measured for each frequency and is plotted in figure 21.

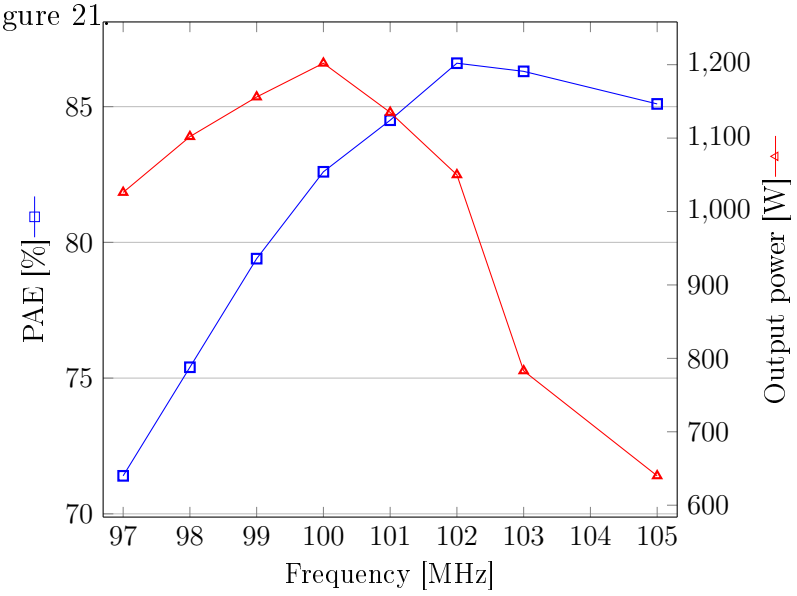

Fig. 21: Power added efficiency and maximum output power as functions of operating frequency.

It can be seen from figure 21 that the measured frequency with the highest power added efficiency is at 102 MHz. Whereas the frequency corresponding to maximum output power is 100 MHz.

This finding motivates some further investigation into the behaviour of the amplifier at 102 MHz.

7.2 102 MHz performance

At 102 MHz the power added efficiency of the amplifier is 86.4% at an power output of 1050 Watts. Figure 22 displays the power added efficiency of the amplifier versus output power and figure 23 displays the gain of the amplifier versus output power at 102 MHz.

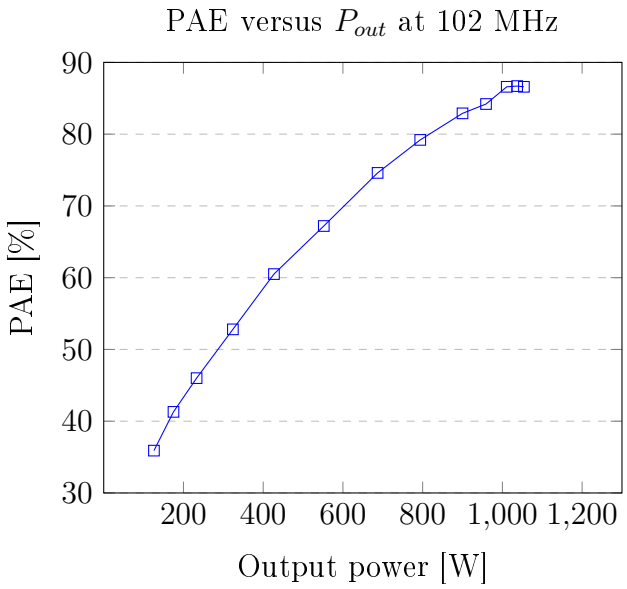

Fig. 22: Power added efficiency as a function of output power measured at 102 MHz

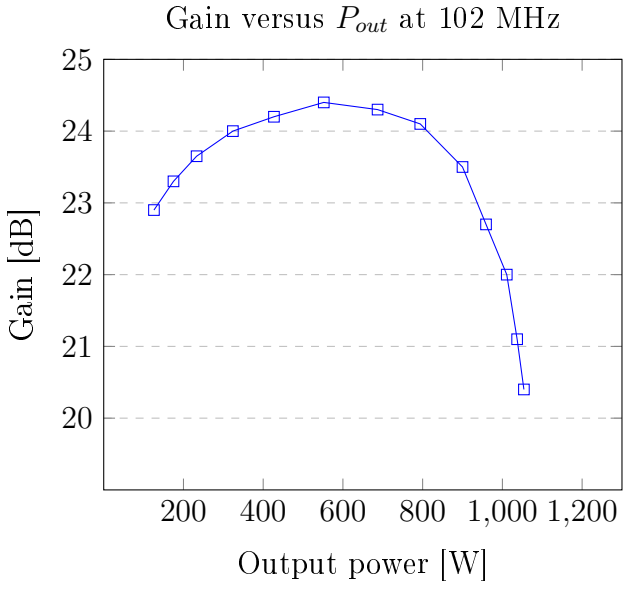

Fig. 23: Power gain as a function of output power measured at 102 MHz

So far we have seen that the voltage waveforms correspond well with the waveforms predicted in simulation. However, the principle of a switch mode amplifier is that of separating the voltage and current waveforms in time.

Therefore it is of interest to perform a simultaneous measurement of the voltage and current waveforms in order to verify this separation of voltage and current.

However measuring the drain source current waveform without interfering with the operation of the amplifier is not trivial.

A possible way to measure the drain current waveform indirectly is to instead measure the gate voltage waveform with the assumption that the drain current should essentially follow the gate voltage. This assumption is verified through simulations of the amplifier. Figure 24 shows a plot of the simulated waveforms of drain voltage, drain current and gate voltage.

The real measurement of the gate and voltage waveforms can be seen in figure 25. The figure serves to show the phase difference between the gate and drain voltage. The gate voltage peaks and consequently the drain current peaks are situated between the drain voltage peaks, as expected from theory and simulation.

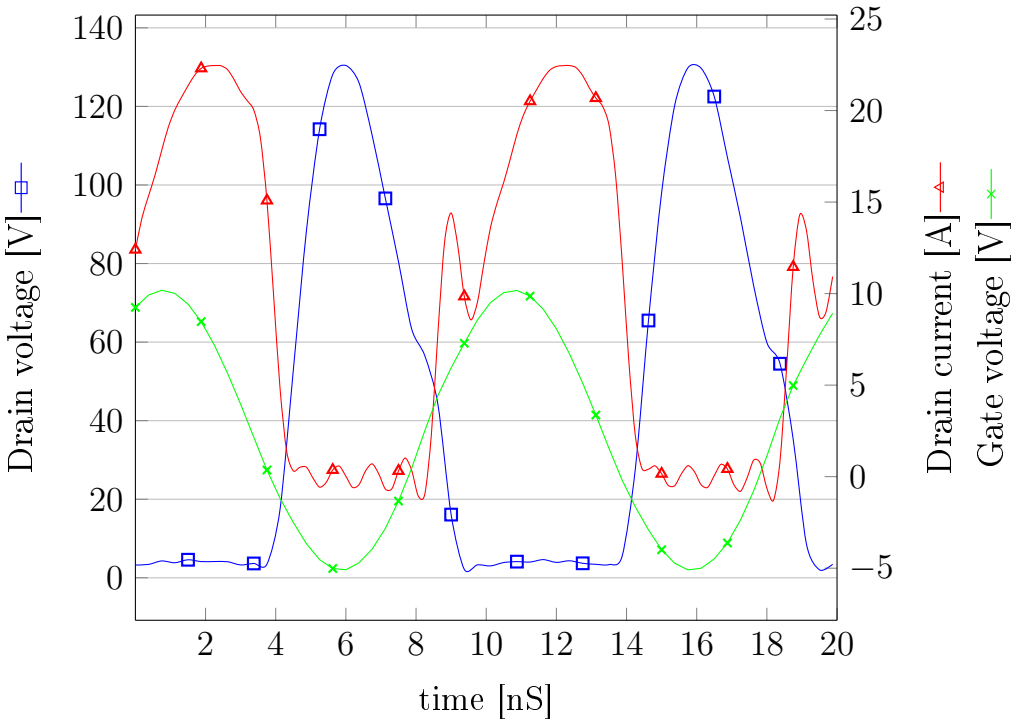

Fig. 24: Simulated waveforms of gate voltage, drain voltage and drain current.

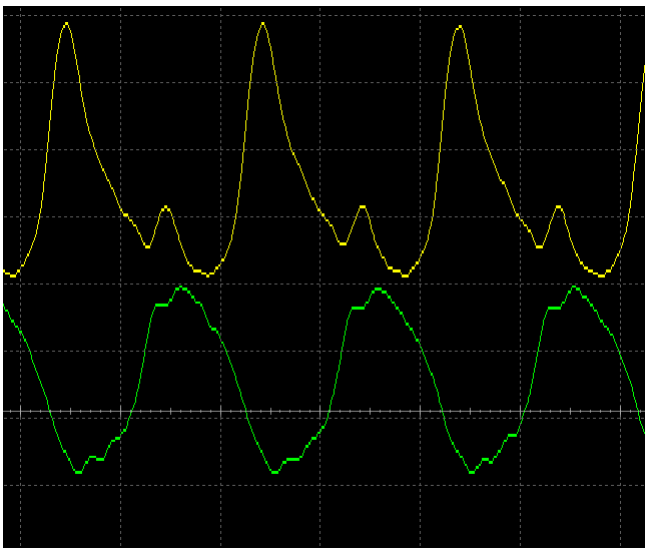

Fig. 25: Measured waveforms of gate voltage and drain voltage waveforms.

7.3 Heating

The heating of the amplifier was monitored during operation with the use of an IR-camera. The heating was higher than anticipated considering the high efficiency of the amplifier. An IR-image of the amplifier in operation is displayed in figure 26.

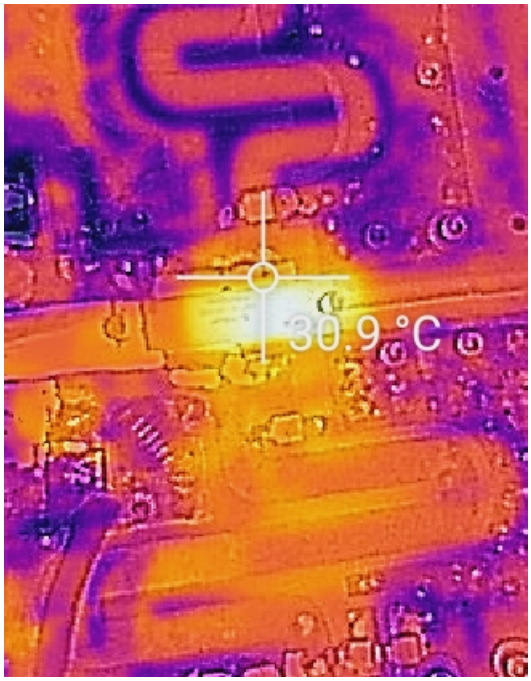

Fig. 26: Infrared image of amplifier while operating.

The reasons for the high heating are related to poor cooling as no heat paste was used between the transistor and heatsink.

7.4 Input matching

The return loss on the input of the amplifier is quite low, c.a 1.5 dB, indicating that the input matching is imperfect. This could be amended at a future time through tuning of the capacitor placements at the input.

8 Conclusions and discussion

The feasibility of realizing a high-power, high-efficiency, class E power amplifier using a simple single-ended design has been demonstrated. The amplifier, based on the power LDMOS-transistor 'BLF188XR', is capable of delivering 1200W peak output power with a power added efficiency of 82% in pulsed power operation at 100 MHz. At 102 MHz operation the peak output power is 1050W with a power added efficiency of 86%.

The design still has some issues, such as the low return loss at the input and the heating of the transistor during operation. The input matching could be improved through tuning of the size and position of the shunt capacitors at the input. However, the input matching does affect the matching at the output, which poses a slight challenge. The heating issues would presumably be alleviated by applying heat-paste to the the transistor.

Although the produced amplifier serves as a proof of concept, there are technical challenges associated with implementation in a cyclotron that are not addressed. For instance that the impedance of a cyclotron is variable.

9 Acknowledgments

I would like to thank Dragos Dancila for giving me the opportunity to do this project and for his continuous support, good ideas, and helpful discussions. Invaluable help was provided by Long Hoang Duc with everything from ADS to measurements. Thanks to Tor Lofnes for his helpful thoughts and input on the experimental setup. I also wish to thank Andreas Lundin for insights on the geometry of transistor biasing. Finally I wish to thank the FREIA laboratory for hosting this master work.

References

[1] Rodriguez, Erik A., et al. "New Dioxaborolane Chemistry Enables [18F]-Positron-Emitting, Fluorescent [18F]-Multimodality Biomolecule Generation from the Solid Phase." Bioconjugate chemistry 27.5 (2016): 1390-1399.

[2] Van Rijs, F. "*Status and trends of silicon LDMOS base station PA technologies to go beyond 2.5 GHz applications*". Radio and Wireless Symposium, 2008 IEEE. IEEE, 2008.

[3] Haapala, Linus, et al. "*Kilowatt-level power amplifier in a single-ended architecture at 352 MHz*". Electronics Letters 52.18 (2016): pp. 1552-1554.

[4] Smirnov, Alexander, et al. "*72 MHz Solid-state Amplifier Power Test*". WEPME008, Proc. of Ipac2014, Dresden, Germany (2014): pp. 2270-2272 .

[5] Ortega-Gonzalez, Francisco Javier. "*High power wideband class-E power amplifier*". IEEE Microwave and Wireless Components Letters 20.10 (2010): pp. 569-571.

[6] Krishnamurthy, K., et al. "*100 W GaN HEMT power amplifier module with> 60% efficiency over 100–1000 MHz bandwidth*". Microwave Symposium Digest (MTT), 2010 IEEE MTT-S International. IEEE, 2010.

[7] Maier, Florian A., et al. "*A GaN-Based 10.1 MHz Class-F-1 300 W Continuous Wave Amplifier Targeting Industrial Power Applications*". Compound Semiconductor Integrated Circuit Symposium (CSICS), 2016 IEEE. IEEE, 2016.

[8] Tang, S., et al. "*A 700W push-pull AlGaN/GaN power amplifier for P-band aerospace application*". Electromagnetics in Advanced Applications (ICEAA), 2016 International Conference on. IEEE, 2016.

[9] Formicone, Gabriele, Jeff Burger, and James Custer. "*A UHF 1-kW solid-state power amplifier for spaceborne SAR*". RF/Microwave Power Amplifiers for Radio and Wireless Applications (PAWR), 2017 IEEE Topical Conference on. IEEE, 2017.

[10] Sokal, Nathan O., and Alan D. Sokal. "*Class EA new class of high-efficiency tuned single-ended switching power amplifiers.*" IEEE Journal of solid-state circuits 10.3 (1975): pp. 168-176.

[11] Raab, Frederick. "*Idealized operation of the class E tuned power amplifier*". IEEE transactions on Circuits and Systems 24.12 (1977): pp. 725-735.

[12] Besser, Les. "*Avoiding RF Oscillation.*" Applied Microwave and Wireless 7 (1995): 44-44.

[13] Ampleon, "*BLF188XR;BLF188XRS - Power LDMOS transistor*" Rev.6 (2015).

[14] Adapted from: https://commons.wikimedia.org/wiki/File:EM_spectrum.sv Retrieved September 4th 2017. Copyright 2007 by Philip Ronan. Adapted with permission.

[15] Pozar, David M. "*Microwave engineering*". John Wiley & Sons, (2012)

[16] Grebennikov, Andrei, Nathan O. Sokal, and Marc J. Franco. "*Switchmode RF and microwave power amplifiers*". Academic Press, 2012.

[17] BLF188XR: Simulation model for ADS 2016. Ampleon. Published 2017-01-16. Available from: http://www.ampleon.com/products/broadcast/0-500-mhz-rf-power-transistors/BLF188XR.html

[18] ADS Class E design equation template. Available from: http://www.keysight.com/find/eesof-how-to-pa-series

[19] Kyung-Whan, Yeom. "*Microwave circuit design*". Pearson (2015). pp 705-717.

[20] TMM Thermoset microwave materials TMM3, TMM4, TMM6, TMM10, TMM10i, TMM13i. Rogers corportation (2015).

A Appendix A

A.1 ADS equations

$$vmax = max(ts(vds)) \tag{8}$$

$$P_{DC} = vccmeas[0] \cdot idc.i[0] \tag{9}$$

$$P_{out} = real(0.5 \cdot V_{out}[1] \cdot conj(iout.i[1])) \tag{10}$$

$$PAE = 100 \cdot real((P_{out} - P_{in})/P_{DC}) \tag{11}$$

$$V_{C1}max = max(ts(vc1)) \tag{12}$$

$$V_{C2}max = max(ts(vc2)) \tag{13}$$

B Appendix B

B.1 Electronics at high frequencies

The everyday AC applications in our home, like vacuum cleaners and toasters operate at a frequency of 50 Hz. An electromagnetic wave with a frequency of 50 Hz has a wavelength of several thousand kilometers. In these types of applications it is safe to assume that the phase of a voltage signal remains unchanged over the physical dimensions of the system, and that the only phase changes that needs to be considered are those that arise from reactive components.

However, when the frequency of an electromagnetic wave increases; its wavelength decreases proportionally and for high enough frequencies the wavelength of the electrical signals in a system will be comparable to the physical dimensions of its components.

At these higher frequencies classical circuit theory breaks down and is generally unable to describe the function of high frequency circuits. This is because classical circuit theory is a simplification of Maxwell's equations and is only valid as long as the wave-nature of the signal is negligible.

This wave-nature of the voltage signal gives rise to a multitude of effects which needs to be taken into consideration. For instance, voltage signals will be reflected at discontinuities in impedance, for example at transition between a conductor and a load.

These effects start becoming significant when the wavelength of the electrical signal is comparable to the electrical system of interest. In our case this will be on the scale of meters which corresponds to frequencies of about a hundred megahertz These are the same frequencies at which standard FM-radio is sent. The part of the electromagnetic spectrum corresponding to these frequencies can be seen marked as "FM-radio" in figure 27.

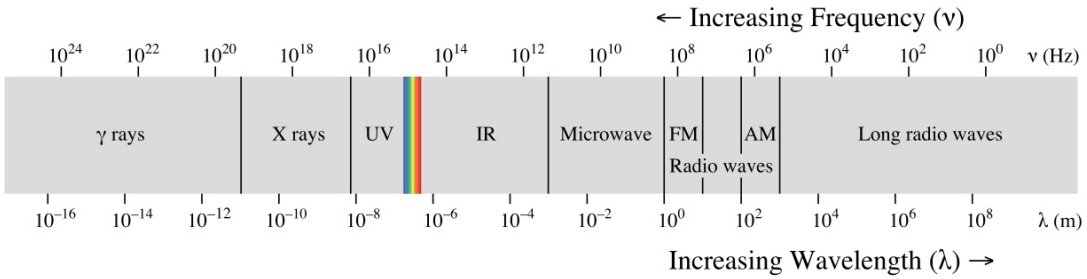

Fig. 27: The electromagnetic spectrum. [14]

The consequence of all this is that since the instantaneous value of voltage and current changes over the length of components, voltages are not necessarily the most useful way of characterizing a circuit. Therefore other parameters such as power, reflection coefficient, and S-parameters are used instead. These concepts will be described further in the following sections.

B.1.1 Transmission lines and distributed elements

Conductors and the dimensions of components are neglected at low frequencies, but since voltages change with distance at high frequencies conductors can have a very significant impact; and are often designed to be crucial components in circuits.

In a high frequency context conductors are referred to as transmission lines. A voltage signal propagating through a transmission line will give rise to a current. The ratio between the voltage and current on the line is its characteristic impedance (denoted Z_0). The characteristic impedance of the transmission line is determined by its dimensions and material properties.

The standard impedance used in most systems is 50 Ohms. It was chosen as a compromise between having good power handling and low losses.

If one wishes to connect a 50 Ohm source with a 50 Ohm load the characteristic impedance of the transmission line will also have to be 50 Ohms or else reflections will arise due to the discontinuity in impedance.

The length of a transmission line will not affect its characteristic impedance. However, the phase of a voltage signal will change with the length of the line. Hence the

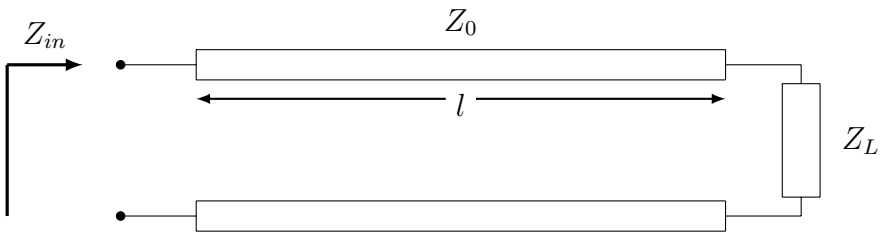

Fig. 28: Input impedance Z_{in} of a transmission line of length l with characteristic impedance Z_0 connected to a load Z_L

length will still affect what impedance is 'seen' at the input of a transmission line, making it crucial in circuit design.

The total input impedance of a transmission line with characteristic impedance Z_0 terminated with a load Z_L is determined by the following expression[15]:

$$Z_{in} = Z_0 \frac{Z_L + jZ_0 \tan(\beta l)}{Z_0 + jZ_L \tan(\beta l)} \tag{14}$$

Where Z_{in} is the input impedance, Z_0 is the characteristic impedance of the transmission line, l is the length of the line, $\beta = \frac{2\pi}{\lambda}$ is the wave number, and Z_L is the load impedance.

This expression allows choosing what impedance is seen from a point by choosing the dimensions of a transmission line.

B.1.2 Reflection Coefficients

As previously mentioned due its wave-nature; a voltage signal will cause reflections at discontinuities in impedance. The ratio of the reflected to the transmitted part of a voltage signal is the reflection coefficient, which acts as a measure of the mismatch in impedances. Reflection coefficients are a very useful concept and is used frequently in RF circuit design.

$$\Gamma = \frac{V_R}{V_I} \tag{15}$$

When designing an RF circuit it is often the case that certain reflection coefficients are desired. For instance it is a very common goal to minimize the magnitude of the

reflection coefficient in order to maximize transmitted power; for instance from an amplifier to a load. Another reason for wanting to minimize the reflection coefficient is that high reflection coefficients can be problematic, since large reflected voltages can damage signal generators, amplifiers and other sensitive equipment.

However there are examples when minimizing the reflection coefficient is not the main goal. For instance if the goal is to maximize efficiency or minimizing noise of an amplifier rather than maximizing the transmitted power. In practice there is often a trade-off when choosing reflection coefficients, and often the most suitable coefficient is a compromise between several goals.

This begs the question, how can reflection coefficients be chosen?

It can be shown that the reflection coefficient at the transition between two impedances Z_1 and Z_2 can be expressed solely in terms of these impedances as [15]:

$$\Gamma = \frac{Z_2 - Z_1}{Z_2 + Z_1} \tag{16}$$

For a voltage signal which transitions from Z_1 to Z_2

So, in order to choose our desired reflection coefficient we need to be able to choose the impedances in our circuit. However, the impedances in a circuit is not free to choose. For example the output impedance of a transistor in an amplifier is determined by the transistor and its biasing conditions, and is often a few ohms. As opposed to a typical load impedance which is 50 Ohms.

By using transmission lines and or lumped components like capacitors and inductors one can make any impedance appear to be any other impedance at the input of an intermediate network. This is known as impedance matching. A network that can match two impedances is called a matching network and it allows a designer to produce a reflection coefficient of choice.

From equation (14) it is possible to design matching networks analytically by finding a solution that transforms the impedance into another.

B.1.3 Impedance matching and the Smith chart

Impedance matching can also be performed graphically using a Smith chart

The Smith chart is a coordinate system which connects the complex reflection coefficients with normalized impedances through the following expression [15]:

$$\Gamma = \frac{z-1}{z+1} \tag{17}$$

Where z is the normalized impedance $\frac{Z}{Z_0}$. The impedances are usually normalized to the characteristic impedance Z_0, which is often 50 Ohms.

A way to understand the Smith chart is to remember that a discontinuity in impedance gives rise to a reflection in voltage. A Smith chart simply maps all possible impedances to their corresponding reflection coefficients given a certain normalization impedance. Negative resistances corresponding to active components lie outside of the chart.

Impedances in the Smith chart are plotted as circles of constant resistance and circle arcs of constant reactance. With the magnitude of resistance and reactance decreasing with increasing radii of the circles.

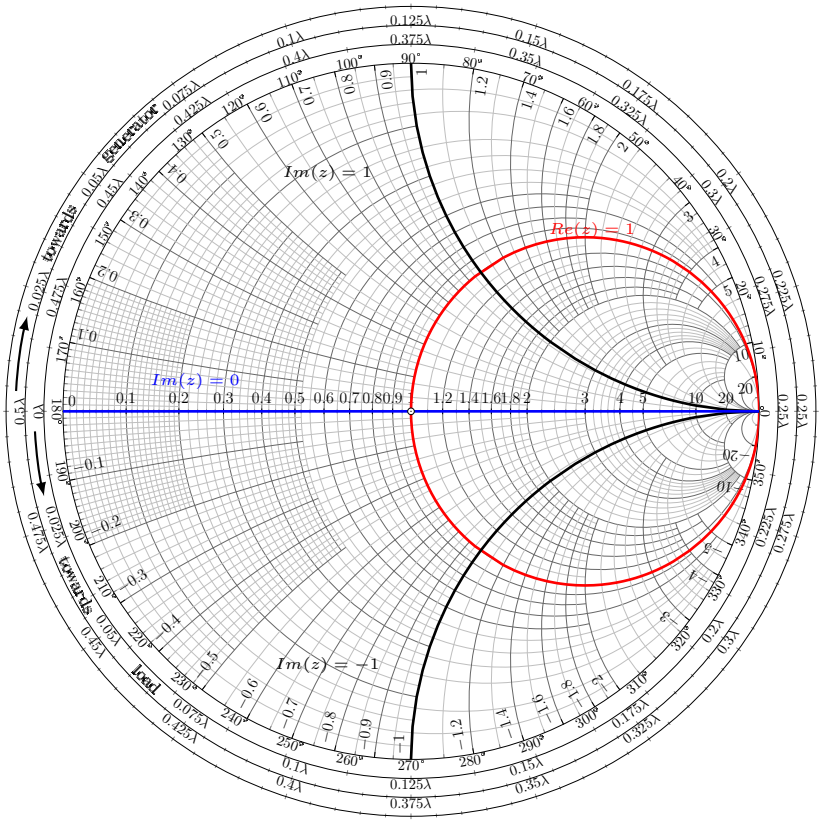

Fig. 29: The Smith chart, a mapping between impedances and reflection coefficients.

The reflection coefficient for a given impedance is found from the intersection of impedance point and constant Γ-circle.

The magnitude of the reflection coefficient is given by the distance from the center of the chart, and its phase is read from the perimeter of the chart.

Since we established earlier that the dimensions of components can change the impedance that is seen from a point, it should come as no surprise that components and their dimensions can be used to move in the Smith chart.

As an example, say that we want to match a 25+j25Ω source to a 50 Ω load for a 1 GHz system. One way of doing this would be to add a series transmission line in order to move clockwise around a circle of constant reflection coefficient until we reach the 50Ω circle of constant resistance. Then add a series capacitance to move counter-clockwise along the 50 Ω constant resistance circle until we reach the 50+j0 Ω point at the center of the chart. It is worth noting that this path is one of an infinite number of possible paths in the Smith chart. Therefore an infinite number of equally valid matching networks could be made.

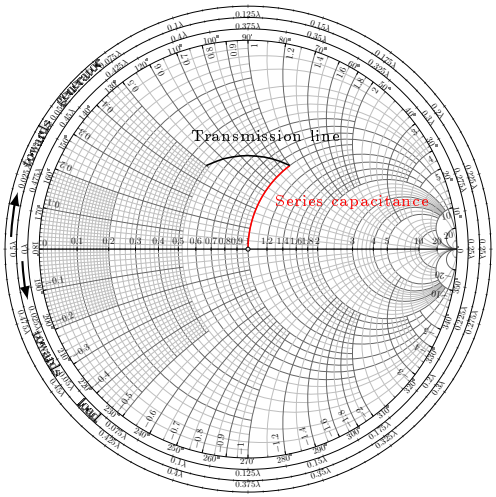

Fig. 30: The impedance matching of a 25 +j25Ω source to a 50Ω load.

The length of the transmission line can be found from the change in angle of the reflection coefficient. We started at an angle of 117° and ended at 64°, which is a difference of 53 degrees. This corresponds to a transmission line length of $\frac{53}{720}\lambda = 0.0736\lambda$. (720° since a voltage signal travels through the transmission line twice)

The size of the series capacitor can be found from the formula of capacitor impedance:

$Z_C = \frac{1}{j\omega C}$ We moved from the point 50 +j50 Ω to 50 + j0 Ω so the impedance of our capacitor is -j50Ω. Thus: $\frac{1}{j\omega C} = -j50\Omega \implies \frac{1}{\omega C} = 50 \implies C = \frac{1}{50\omega} = 3.18pF$

Consequently our impedance matching network would look as depicted in figure 31.

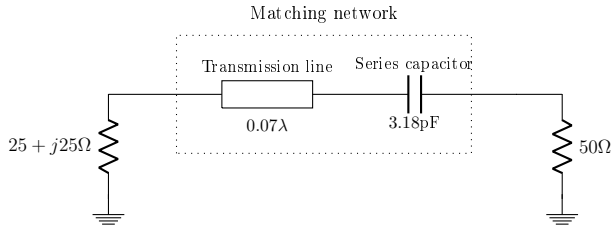

Fig. 31: Matching network between the impedances 25 +j25Ω and 50Ω for the frequency 1 GHz

B.1.4 Scattering parameters

A useful concept in RF engineering is scattering parameters or 'S-parameters'.

With the use of S-parameters any electrical system can be described as an N-port. An N-port is an unknown network or a 'black box' featuring N pairs of terminals referred to as ports. For a voltage signal that enters a port some of the signal will be reflected back to that port, some parts may exit at other ports. Exactly which paths the signal take within the black box is not essential and system is completely described by the voltages seen on each port when a voltage is introduced at each other port.

More specifically an S-parameter S_{xy} is defined as the ratio between the voltage seen at port x for a voltage entering port y. With the added condition that all other ports are terminated in matched loads so as to not contribute to the signal via additional reflections.

The S-parameters are complex numbers since they take into account possible changes in both the amplitude and the phase of the voltage.

An N-port system can then be described using an N×N S-parameter matrix. The columns of the matrix each correspond to an input port and the rows to an output port, so that the element in column x and row y corresponds to the s-parameter S_{xy}.

The elements on the diagonal of the S-matrix are reflection coefficients, since they

describe what voltage is seen returning to the same input into witch the voltage signal entered. The off-diagonal elements are transmission coefficients since they describe what voltage is seen at one input when a voltage signal enters another input.

A special case of particular interest is that of the 2-port system. This is because an amplifier can be seen as a two port with one input port and one output port.

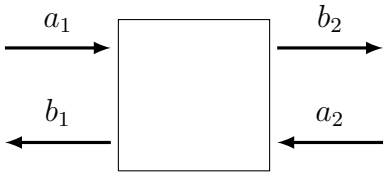

Fig. 32: A two-port network with incoming voltages a1 and a2, and outgoing voltages b1 and b2

The incoming and outgoing voltage signals of the two port system can be related using the systems S-matrix as follows:

$$\begin{pmatrix} a_1 \\ a_2 \end{pmatrix} \begin{pmatrix} S_{11} & S_{12} \\ S_{21} & S_{22} \end{pmatrix} = \begin{pmatrix} b_1 \\ b_2 \end{pmatrix}$$

In the context of amplifiers the S-parameters can be interpreted in the following way:

- S_{11} - Input reflection coefficient
- S_{12} - Reverse isolation parameter
- S_{21} - Voltage gain
- S_{22} - Output reflection coefficient

The parameter S_{12} requires some further explanation: It is a measure of how much of a voltage signal that is transmitted from the output to the input of the amplifier. An ideal amplifier would have its input and output perfectly isolated from each other and would therefore have a S_{12} parameter equal to zero. Devices with a zero reverse isolation parameter are referred to as being 'unilateral'. However, in real devices we need to consider the bidirectional case, and the S_{12} parameter is of importance when determining the stability of an amplifier.